Turkish Journal of Electrical Engineering & Computer Sciences

http://journals.tubitak.gov.tr/elektrik/

Research Article

Turk J Elec Eng & Comp Sci
(2020) 28: 1599 – 1611

doi:10.3906/elk-1909-20

Two novel radar detectors for spiky sea clutter with the presence of thermal noise and interfering targets

Nouh GUIDOUM[1,*], **Faouzi SOLTANI**[1], **Amar MEZACHE**[2]
[1]Département d'Electronique, Laboratoire Signaux et Systèmes de Communication,
Université des Frères Mentouri Constantine 1, Constantine, Algeria
[2]Département d'Electronique, Université Mohamed Boudiaf de M'sila, M'sila, Algeria

Received: 03.09.2019 • **Accepted/Published Online:** 02.03.2020 • **Final Version:** 08.05.2020

Abstract: In the context of noncoherent detection and high-resolution maritime radar system with low grazing angle, new Constant False Alarm Rate (CFAR) decision rules are suggested for two Compound Gaussian (CG) clutters namely: The K distribution and the Compound Inverse Gaussian (CIG) distribution, which are considered among the most appropriate models for sea clutter. The proposed decision rules are then modified to deal with the presence of thermal noise and interfering targets. The proposed detectors are investigated on the basis of synthetic data as well as real data of the IPIX radar database. The obtained results exhibit a high probability of detection as well as an excellent false alarm rate regulation especially for spiky clutter.

Key words: Maritime radar, detection, compound Gaussian, thermal noise, interfering targets

1. Introduction

To ensure a good performance of a radar system with high resolution, the CFAR property must be preserved with respect to all types of background heterogeneities. In a maritime radar surveillance environment, the power of the sea clutter can undergo severe random variations due to sea state, wind speed and wave height [1], which generate a significant increase in the rate of false alarm and makes the mission of detection of small targets like the periscope of the submarine or small boats a difficult task. In addition to these problems, sea clutter deviates from normality [2, 3]. To alleviate these problems, non-Gaussian models of sea clutter are strongly desired and are the subject of many experimental studies. Several distributions have been suggested as an alternative to the Gaussian model for describing the intensity statistics of the sea clutter. The K distribution provides a compound representation that includes the speckle, which represents the fast fluctuating component associated to capillarity waves and the underlying mean or the texture which is the slowly fluctuating component related to gravity waves [4]. More recently the CIG distribution where the texture is modeled by an inverse Gaussian distribution showed a good adaptation with sea clutter [5]. These models have been modified to include the thermal noise to be able to adapt with impulsive clutter and heavy echoes.

Noncoherent radar systems are widely used for analyzing sea clutter and have been an intensive research topic for many years. Goldstein suggested the log-t CFAR detector for two distributions, namely; lognormal and Weibull clutters. This detector proved to insure the CFAR property for the two mentioned distributions [6]. Weber and Haykin suggested a modification of the ordered statistic OS-CFAR which is designed to be

*Correspondence: soltani.faouzi@umc.edu.dz

CFAR for two-parameter distributions with unknown average power and unknown skewness. This detector is CFAR for the lognormal, Weibull, and Gamma distributions [7]. For the K distribution, Armstrong and Griffiths examined the detection performance in correlated clutter for three different CFAR detectors, the cell averaging (CA), greatest of (GO) and order statistics (OS) CFAR. These detectors suffer from a significant loss in detection relative to the ideal CFAR especially in the case of spiky clutter [8]. Conte et al, studied two different methods: first, they perform a Neyman-Pearson detector, based on complete learning of the signal fluctuation law. This study cannot be applied in real situations, because the threshold imposes the knowledge of the target power. The second study depends on the generalized likelihood ratio optimization strategy. This detector achieves the CFAR property and the threshold does not require any knowledge of the clutter distribution [9]. Zhou et al suggested a new CFAR detector in nonhomogeneous Gamma clutter. The threshold is estimated by the weighted amplitude iteration of the samples in the reference cells by adding the advantages of the CA-CFAR, GO-CFAR and OS-CFAR detectors. The performance of this method approaches that of the CA-CFAR in homogeneous Gamma clutter with a known shape parameter. This approach performs well in a nonhomogeneous environment with the appropriate weighting factors, but suffers from a significant loss in detection in the CA, GO and OS-CFAR and shows an important increase in the false alarm rate [10]. Norouzi et al suggested a new CFAR algorithm based on goodness-of-fit (GoF) for heavy-tailed Weibull and log normal distributions. In spiky clutter and in the presence of interfering targets, this detector is superior to the conventional CFAR detector based on binary integration [11]. In the K distributed sea clutter, Watts et al examined the performance of cell-averaging CFAR. In the case of spiky clutter or when the texture (underlying mean) of clutter is uncorrelated, the CA-CFAR suffers from a significant loss. It has been found that the use of short cell-average lengths or an increase in the thermal noise in the radar system leads to a CFAR gain [12]. Weinberg and Alexopoulos proposed a dual order statistic using the Pareto clutter model which achieves the CFAR property, then they examined the performance of this detector in the case of the presence of interfering targets and clutter transitions [13]. Weinberg and Glenny explored the log-t detector using the Pareto clutter model which achieves the CFAR property [14]. For the noncoherent radar system, we propose two detectors for sea clutter models with the presence of thermal noise. We show that these two detectors conserve the CFAR property for the two CG distributions under consideration especially for spiky clutter situations. Then, we modify the proposed detectors to deal with the presence of thermal noise and interfering targets. The robustness of the proposed detectors is then validated using real data of the IPIX radar database. The paper is structured as follows: In Section 2, we describe the two proposed detectors, then we briefly recall the expressions of the K plus thermal noise and the Compound Inverse Gaussian (CIG) plus thermal noise and we present some results of the variations of the Probability of false alarm (P_{fa}) versus the threshold for each detector. In Section 3, we study the robustness of the suggested detectors in the case of the presence of interfering targets in the reference cells and we show some results in terms of P_{fa} and the Probability of detection (P_d). In the next section, we examine the performance of the two detectors using the IPIX real data. In the final section, we give a conclusion for this study.

2. Proposed detectors: The max-min detector and the var-max-min detector

The two proposed detectors shown in Figure 1 are designed to be CFAR and able to provide a high probability of detection in the case of the presence of thermal noise and interfering targets. The content of each cell is obtained by sampling the signal received at the output of the square law envelope detector. The obtained samples are

stored in a shift register and the detection test in each cell uses a reference window of N cells adjacent to the cell under test (CUT) which provide a local estimate of the clutter level. The sliding of this window along the register of cells makes it possible to cover the entire radar range. The suggested thresholds were found using the trial and error method and the choice of the number of reference cells for both detectors were found after intensive testing for several values from 2 to 32 cells. The best performances in terms of false alarm regulation of the suggested detectors are obtained for a number equal to 2, which is useful regarding the calculation time and the stationarity of clutter. The principle of our detectors is based on a binary decision-making. Indeed, this binary decision is performed by comparing the content of the CUT with an adaptive detection threshold, denoted T_h to choose between two statistical assumptions: H_0 for the null hypothesis (absence of the target of interest) and H_1 for the alternative hypothesis (presence of the target of interest). Monte Carlo simulations are performed to investigate the suggested decision rules for the CG models: The K and CIG distribution, with the consideration of the presence of thermal noise for the two distributions.

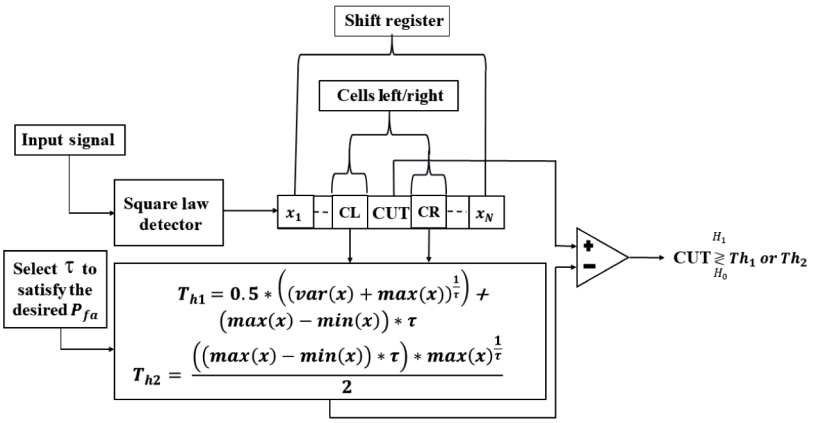

Figure 1: Block diagram of the two proposed detectors.

The decision rules corresponding to the (Var-Max-Min) detector and the (Max-Min) detector are based on miscellaneous statistics, the variance, the maximum and the minimum value of the reference cells. The threshold of the first detector is given by:

$$T_{h1} = 0.5 * \left((var(x) + max(x))^{\frac{1}{\tau}}\right) + (max(x) - min(x)) * \tau. \tag{1}$$

The threshold of the second detector is given by:

$$T_{h2} = \frac{((max(x) - min(x)) * \tau) * max\,(x)^{\frac{1}{\tau}}}{2}. \tag{2}$$

2.1. The K distribution plus thermal noise

The K-distribution with thermal noise is supposed to have two components, a fast fluctuating component, called speckle and represented by the random variable X and a slowly varying component, called the texture (underlying mean) and represented by random variable Y. From experimental results, it was shown that the probability density function (pdf) of each components is expressed respectively by an Exponential distribution

and a Gamma distribution [4]:

$$f_{X|Y}(x|y) = \frac{1}{p_n + y} exp\left(-\frac{x}{p_n + y}\right), \tag{3}$$

$$f_Y(y) = \frac{b^\nu}{\Gamma(\nu)} y^{\nu-1} exp\left(-by\right), \tag{4}$$

where ν is the shape parameter, b is the scale parameter and $(p_n = 2\sigma^2)$ is the power of thermal noise. The intensity of the K distribution plus thermal noise is given by [4]:

$$f_X(x) = \frac{b^\nu}{\Gamma(\nu)} \int_0^\infty \frac{y^{\nu-1}}{p_n + y} exp\left(-\frac{x}{p_n + y} - by\right) \mathrm{d}y. \tag{5}$$

Putting $p_n = 0$ leads to the K distribution without thermal noise [4]:

$$f_X(x) = \frac{2b^{\frac{\nu+1}{2}} x^{\frac{\nu-1}{2}}}{\Gamma(\nu)} K_{\nu-1}(2\sqrt{bx}), \tag{6}$$

where $K_{\nu-1}(.)$ represents the modified Bessel function of the second kind, and $\Gamma(.)$ is the Gamma function.

2.2. The compound inverse Gaussian plus thermal noise distribution

The CIG distribution plus thermal noise is modeled by two components, where the texture component is expressed by an inverse Gaussian distribution [5]:

$$f_{X|Y}(x|y) = \frac{x}{p_n + 2y^2/\pi} exp\left(-\frac{x^2}{p_n + 4y^2/\pi}\right), \tag{7}$$

$$f_Y(y) = \frac{\lambda^{1/2}}{\sqrt{2\pi} y^{3/2}} exp\left(-\lambda \frac{(y-\mu)^2}{2\mu^2 y}\right), \tag{8}$$

where λ is the shape parameter, μ is the mean parameter and $(p_n = 2\sigma^2)$ is the power of thermal noise. The intensity of the CIG distribution plus thermal noise is given by [5]:

$$f_X(x) = \int_0^\infty \frac{x}{p_n + 2y^2/\pi} exp\left(-\frac{x^2}{p_n + 4y^2/\pi}\right) \times \frac{\lambda^{1/2}}{\sqrt{2\pi} y^{3/2}} exp\left(-\lambda \frac{(y-\mu)^2}{2\mu^2 y}\right) dy. \tag{9}$$

Putting $p_n = 0$ leads to the CIG distribution without thermal noise.

2.3. False alarm regulation of the proposed detectors in the CG clutter plus thermal noise

In this subsection, we show the variations of P_{fa} versus the threshold factor τ for the two proposed detection schemes for the two clutter distributions listed above. To undertake these simulations, we use the MATLAB tool and the following assumptions: Noncoherent detectors, the variations of P_{fa} from 0 to 10^{-4} with representation in logarithmic base 10, different values of shape and scale parameters. The range for the shape parameter for the two distributions under consideration varies from 0.01 which corresponds to a spiky clutter (agitated sea state) to 6 for ν and 10 for λ which corresponds to a calm sea state. The scale parameters β and μ are set

equal to 1 to 4 to represent different clutter power. The number of independent Monte Carlo runs is set to 10^7 and the thermal noise power $p_n = 2\sigma^2$ is set to 2 dB.

For the Max-Min detector, Figure 2 shows the variation of P_{fa} from values close to 0 to –4 versus the threshold factor τ for the K distribution clutter with different values of shape and scale parameters. We observe that almost all curves overlap with each other without any deviations even when the clutter becomes spiky $\nu \geq 0.01$. The same pattern is observed for the CIG distribution with $\lambda \geq 0.1$ in Figure 3. The two tests prove that the Max-Min detector attain the CFAR property independently of the shape and scale parameters. We also note from the two experiments that the presence of thermal noise does not affect the robustness of the proposed first detector.

On the other hand, we repeated the same tests with the same parameters for the Var-Max-Min detector. We show the variations of P_{fa} against the threshold factor τ for the CG clutter models listed above in Figures 4 and 5. It is clear from the two experiments that all the curves almost coincide with each other. This mean that the Var-Max-Min detector keeps the CFAR property for the CG models with $\nu \geq 1$ and $\lambda \geq 0.1$, also the thermal noise does not affect the false alarm regulation.

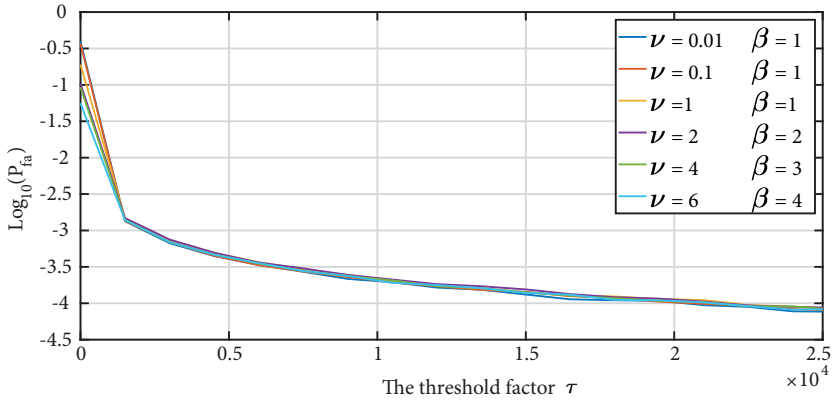

Figure 2: Variation of P_{fa} of the Max-Min detector versus the threshold factor τ for the K distribution.

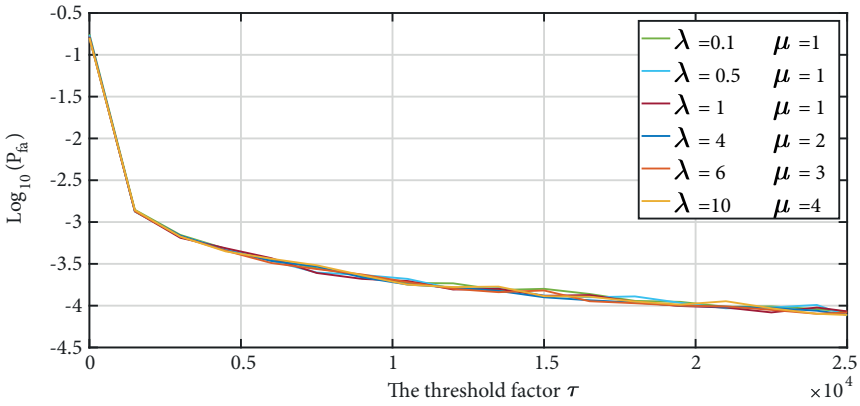

Figure 3: Variation of P_{fa} of the Max-Min detector versus the threshold factor τ for the CIG distribution.

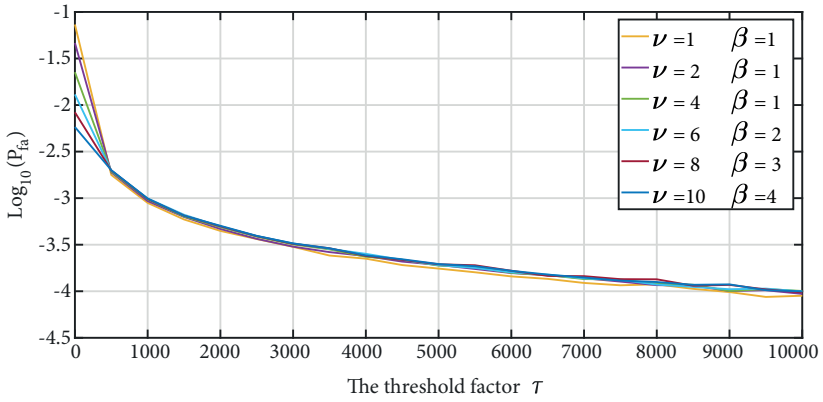

Figure 4: Variation of P_{fa} of the Var-Max-Min detector versus the threshold factor τ for the K distribution.

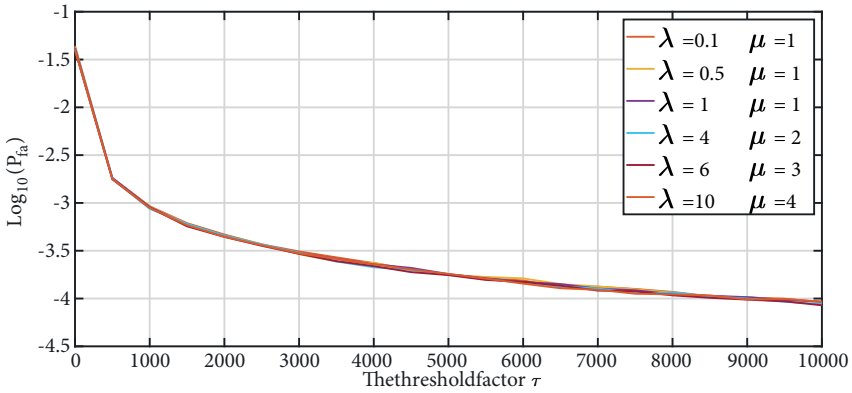

Figure 5: Variation of P_{fa} of the Var-Max-Min detector versus the threshold factor τ for the CIG distribution.

3. Simulation results

In this section, we analyze the detection performance of the two decision rules with the consideration of the presence of a primary target of type Swerling I incorporated in CG clutter in the case of the presence of thermal noise. Then, we study the robustness of P_{fa} regulation in the case of the presence of thermal noise and two interfering targets in the reference cells.

3.1. Probability of detection (P_d) in CG clutter

The following assumptions are considered: The Signal-to-Clutter Ratio (SCR) varies from 0 to 45 dB, the scale parameter set to 1 and $P_{fa} = 10^{-3}$.

We illustrate P_d for the first proposed detector in CG clutter models plus thermal noise. Figure 6 shows P_d versus the SCR in the K distribution clutter, which starts from small values of $\nu \geq 0.01$. We observe that the detection curves are superimposed and indicate that increasing the shape parameter induces an increase in detection. According to the design of the proposed detector, which is based only on two reference cells when estimating the level of clutter, the Max-Min detector provides a high detection performance.

In Figure 7, we repeat the same simulations for the CIG and the same pattern is observed even for the case of spiky clutter $\lambda \geq 0.1$. From the two tests, the presence of thermal noise does not affect the detection performance of the Max-Min detector.

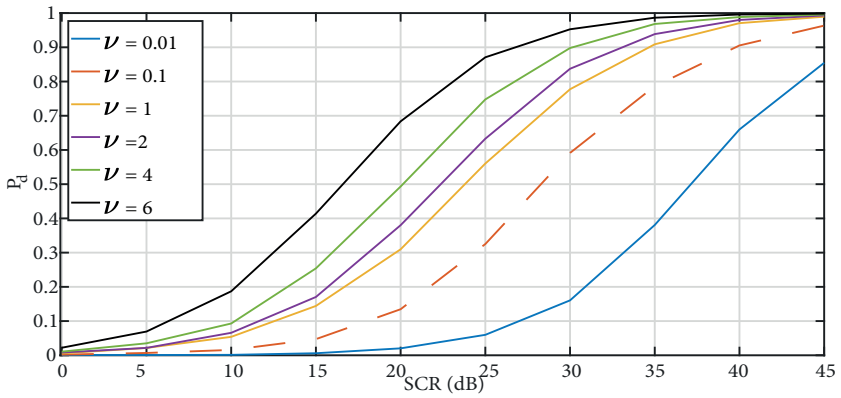

Figure 6: P_d of the Max-Min detector versus the SCR the K distribution.

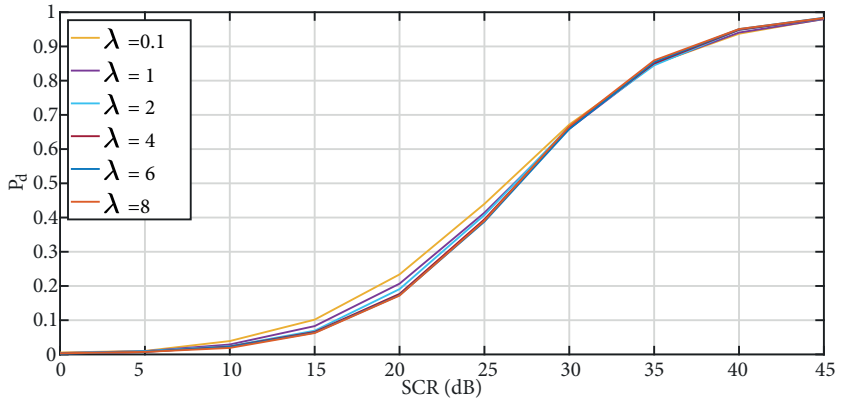

Figure 7: P_d of the Max-Min detector versus the SCR for the CIG distribution.

We repeat the same simulations with the same parameters for the Var-Max-Min detector. We show the variation of P_d versus SCR for CG clutter models mentioned above in Figures 8 and 9 respectively. Through the obtained results, it is clear that this detector provides high detection performance. This means that the second proposed detector keeps the performance of detection for the CG models.

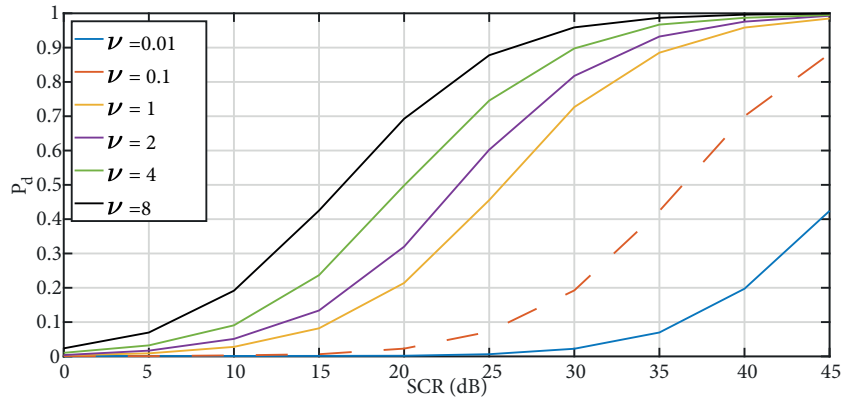

Figure 8: P_d of the Var-Max-Min detector versus the SCR the K distribution.

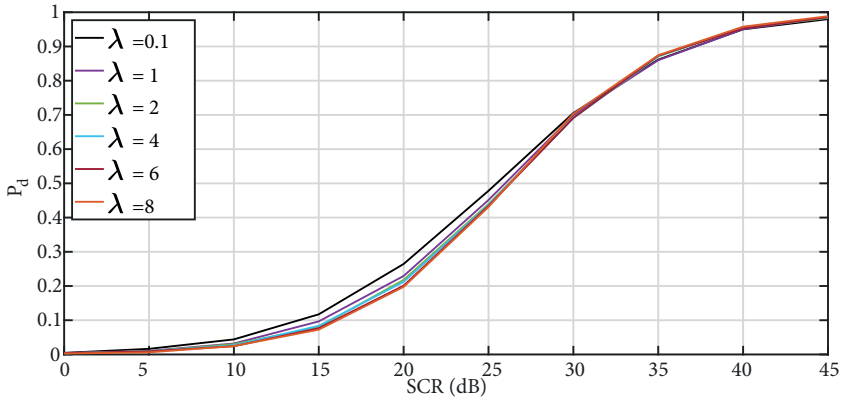

Figure 9: P_d of the Var-Max-Min detector versus the SCR for the CIG distribution.

Finally, in Figure 10 we compare P_d for the two proposed detectors for the distribution K. We observe that for the different values of the shape parameter, the Max-Min detector performs better than the Var-Max-Min detector especially for spiky clutter $\nu = 0.01$ and $\nu = 0.1$.

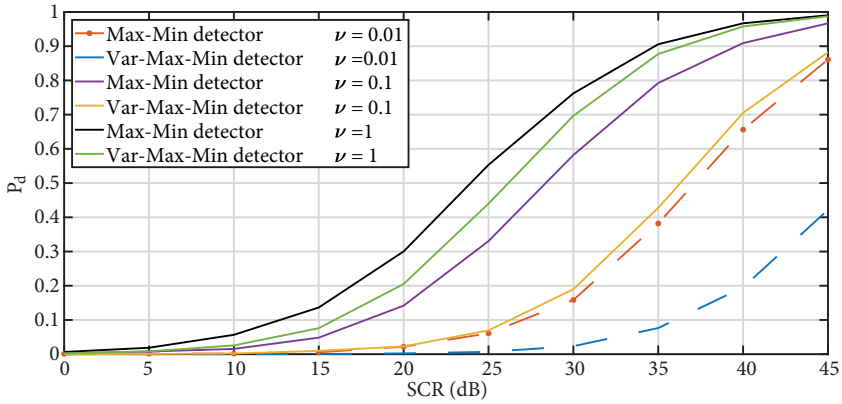

Figure 10: Comparison of P_d between the proposed detectors.

3.2. False alarm regulation of the proposed detectors in CG clutter and interfering targets

In this subsection, we study the effect of the presence of two interfering targets in the reference window on the proposed detectors performance. To test the robustness of the proposed detectors in the case of the presence of one or more interfering targets in the reference window, we modified the first version of the suggested detectors to deal with the presence of interfering targets. Each detector uses four reference cells instead of two, then these cells are arranged in an ascending order to acquire $X_{(1):(4)}$, then the two largest samples are censored, which means that these detectors can handle up to two interfering targets. Each threshold is calculated using the other two samples in the same manner as (1) and (2). To perform this work, we use the same assumptions mentioned above, considering that the interfering targets are supposed to fluctuate according to the Swerling I model and the Interference-to-Clutter Ratio (ICR) is assumed to be equal to 20 dB.

For the K distribution Figure 11 shows the changes of P_{fa} against the threshold factor τ. It is clear that almost all curves overlap, which means that the CFAR property is preserved. For the CIG distribution, the detector also keeps the CFAR characteristic as shown Figure 12.

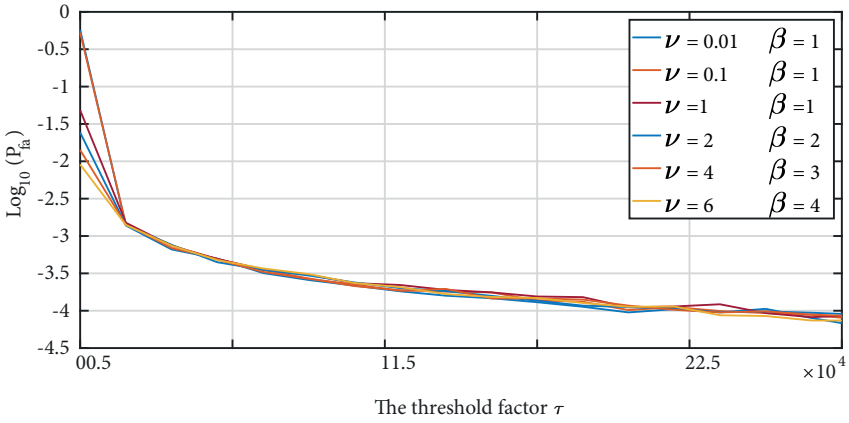

Figure 11: Variation of P_{fa} of the Max-Min detector versus the threshold factor τ for the K distribution plus thermal noise and two interfering targets.

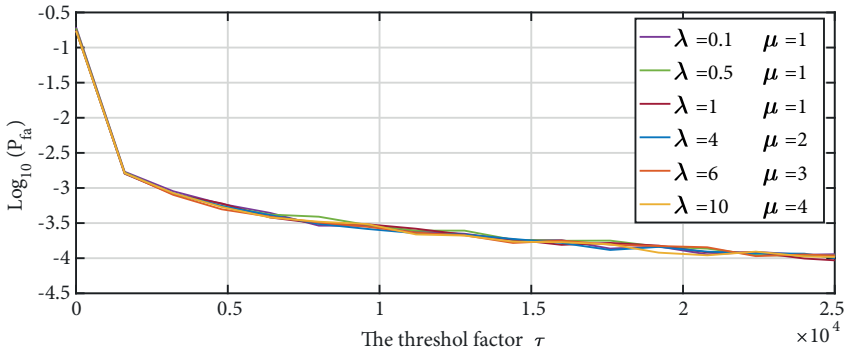

Figure 12: Variation of P_{fa} of the Max-Min detector versus the threshold factor τ for the CIG distribution plus thermal noise and two interfering targets.

We repeat the same simulations with the same parameters for the Var-Max-Min detector. We show the variations of P_{fa} against the threshold factor τ for CG clutter models in Figures 13 and 14 respectively. The same patterns are observed for the K and CIG distributions where all the curves almost match with each other. From the obtained results, the proposed detectors regulate the P_{fa} in an acceptable manner which means that the presence of interference targets in the reference window do not affect the robustness of the proposed detectors.

4. Experimental results

To evaluate the performance of the two suggested detectors with real data, we use a large set of experimental data collected by the McMaster IPIX (Intelligent Pixel processing X-band) radar at the east coast of Canada, in Dartmouth, Nova Scotia. Three range resolutions are available: 3m, 15m and 30m with two modes of polarization of radar antenna HH and VV. The number of reference cells is 34 and the number of pulses per cell distance is 60000.

Figures 15 and 16 depict the variations of P_{fa} from 0 to 10^{-3} for the two detectors. For the three resolutions: high, average and low resolution, 3m, 15m and 30m with two polarization modes HH and VV, we note that almost all curves overlap without any deviations. The experimental variations of P_{fa} of the actual

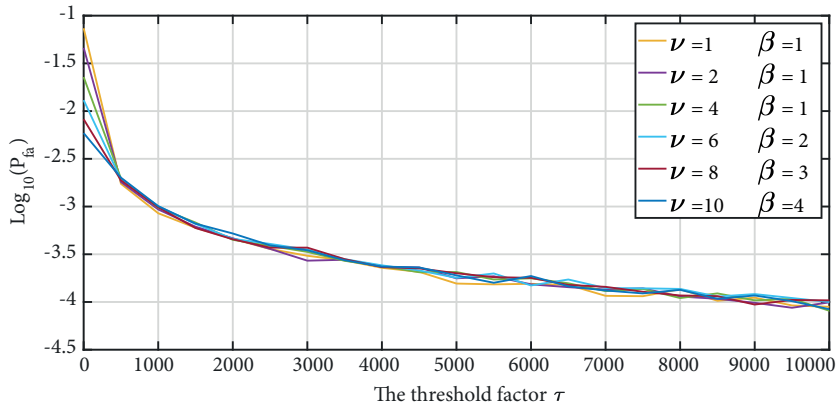

Figure 13: Variation of P_{fa} of the the Var-Max-Min detector versus the threshold factor τ for the K distribution plus thermal noise and two interfering targets.

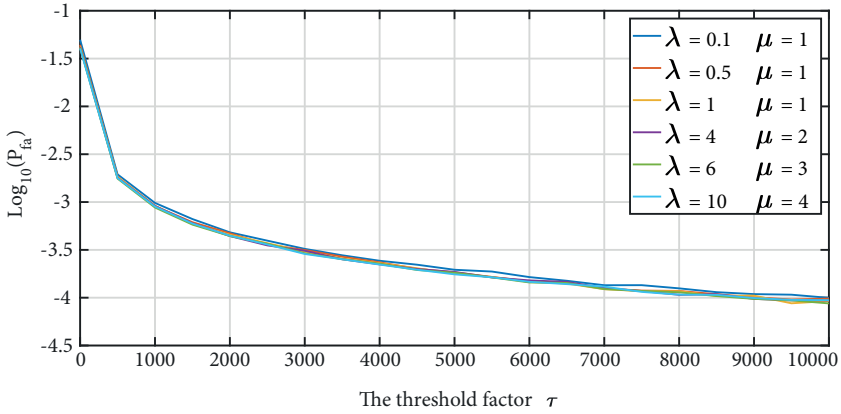

Figure 14: Variation of P_{fa} of the Var-Max-Min detector versus the threshold factor τ for the CIG distribution plus thermal noise and two interfering.

IPIX data are similar to the theoretical variations obtained from the CG clutter in the case of the presence of thermal noise and interfering targets, with almost the same threshold factor to obtain a desired P_{fa}. This means that both detectors maintain the CFAR property successfully.

Finally for P_d, Figure 17 and 18 show the detection curves for each resolution. As expected, all detection curves attain 1 for an SCR around 45 dB. This means that the proposed detectors maintain the same detection performance for experimental data successfully.

5. Conclusions

In this paper, we have proposed two new CFAR detectors operating in sea clutter modeled by CG distributions. We have assumed the presence of thermal noise and interfering targets. The two detectors employ two reference cells to set up the detection threshold. The robustness of the proposed detectors is illustrated through numerical simulations performed on the CG models as well on actual IPIX radar data. In the case of the presence of the thermal noise, both detectors maintain a good performance in terms of false alarm regulation. We have also tested these detectors in the case where two interfering targets are present by modifying the detection algorithm

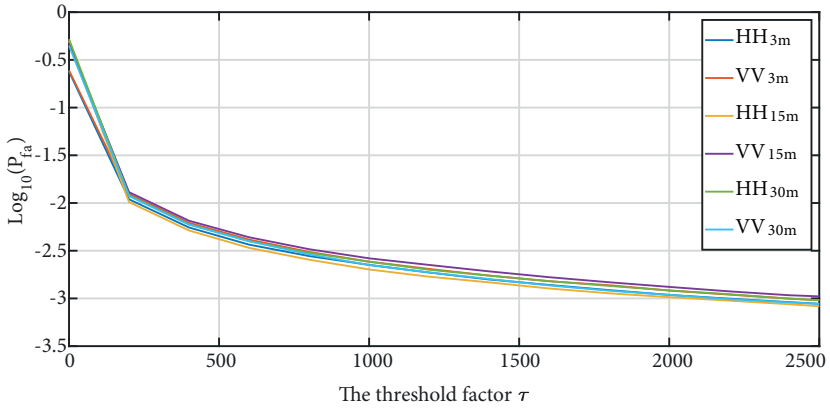

Figure 15: Variation of P_{fa} of the Max-Min detector versus the threshold factor τ for the actual data IPIX.

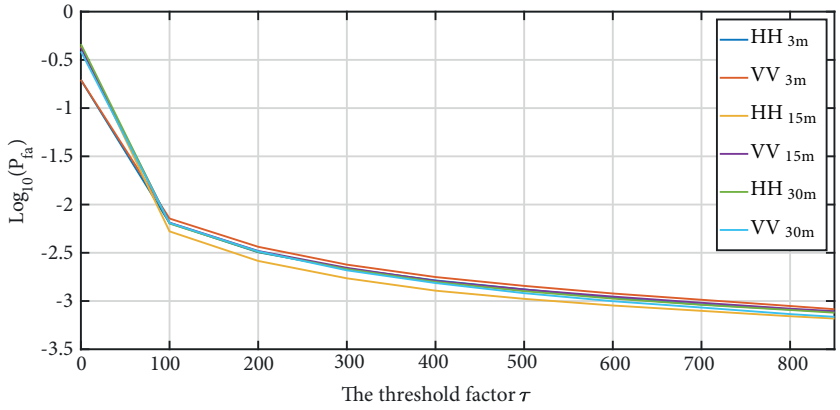

Figure 16: Variation of P_{fa} of the Var-Max-Min detector versus the threshold factor τ for the actual data IPIX.

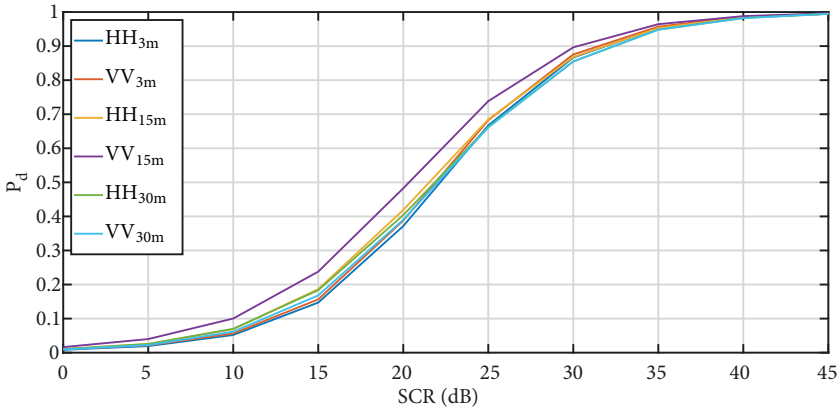

Figure 17: Variation of P_{fa} of the Max-Min detector versus the threshold factor τ for the actual data IPIX.

and the they proved to be robust. To validate these two detectors, we applied real data from the IPIX data base and the results are similar to those obtained by synthetic data. Finally, it is worth pointing out that since the decision operation uses only two reference cells, these detectors are appropriate for real time applications.

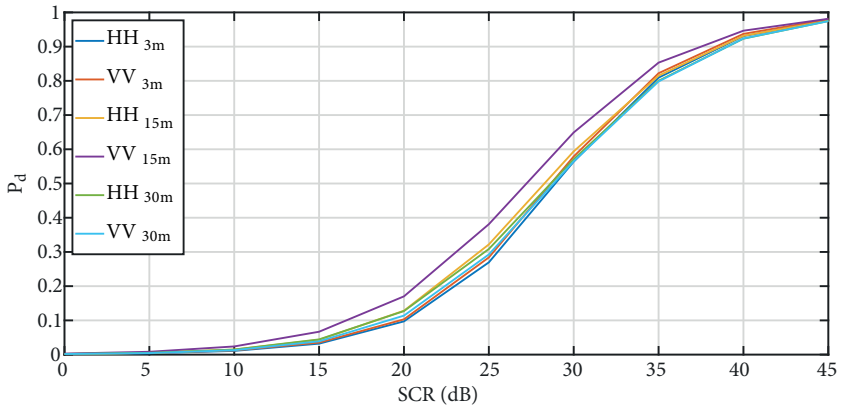

Figure 18: Variation of P_{fa} of the Var-Max-Min detector versus the threshold factor τ for the actual data IPIX.

References

[1] Jayaprakash A, Reddy GR, Prasad N. Small Target Detection Within Sea Clutter Based on Fractal Analysis. Procedia Technology 2016; 24: 988-995. doi: 10.1016/j.protcy.2016.05.217

[2] Farina A, Gini F, Greco M, Verrazzani L. High resolution sea clutter data: statistical analysis of recorded live data. IEE Proceedings - Radar, Sonar & Navigation 1997; 144 (3): 121. doi:10.1049/ip-rsn:19971107

[3] Chan H. Radar sea-clutter at low grazing angles. IEE Proceedings F Radar and Signal Processing 1990; 137 (2): 102. doi:10.1049/ip-f-2.1990.0015

[4] Ward KD, Tough RJA, Watts S. Sea clutter: scattering, the K distribution and radar performance. Stevenage, Herts, United Kingdom 2013. Institution of Engineering and Technology.

[5] Mezache A, Soltani F, Sahed M, Chalabi I. Model for non-rayleigh clutter amplitudes using compound inverse gaussian distribution: an experimental analysis. IEEE Transactions on Aerospace and Electronic Systems 2015; 51 (1): 142-153. doi: 10.1109/taes.2014.130332

[6] Goldstein G. False-Alarm Regulation in Log-Normal and Weibull Clutter. IEEE Transactions on Aerospace and Electronic Systems 1973; AES-9 (1): 84-92. doi: 10.1109/taes.1973.309705

[7] Weber P, Haykin S. Ordered Statistic CFAR Processing for Two-Parameter Distributions with Variable Skewness. IEEE Transactions on Aerospace and Electronic Systems 1985; AES-21 (6): 819-821. doi: 10.1109/taes.1985.310668

[8] Armstrong B, Griffiths H. CFAR detection of fluctuating targets in spatially correlated K-distributed clutter. IEE Proceedings F Radar and Signal Processing 1991; 138 (2): 139. doi: 10.1049/ip-f-2.1991.0020

[9] Conte E, Lops M, Ricci G. Incoherent radar detection in compound-Gaussian clutter. IEEE Transactions on Aerospace and Electronic Systems 1999; 35 (3): 790-800. doi: 10.1109/7.784052

[10] Zhou W, Xie J, Li G, Du Y. Robust CFAR Detector With Weighted Amplitude Iteration in Nonhomogeneous Sea Clutter. IEEE Transactions on Aerospace and Electronic Systems 2017; 53 (3): 1520-1535. doi: 10.1109/taes.2017.2671798

[11] Norouzi Y, Gini F, Nayebi M, Greco M. Non-coherent radar CFAR detection based on goodness-of-fit tests. IET Radar, Sonar & Navigation 2007; 1 (2): 98. doi: 10.1049/iet-rsn:20060032

[12] Watts S, Ward K, Tough R. CFAR loss and gain in K-distributed sea-clutter and thermal noise. IET International Conference on Radar Systems 2007. doi: 10.1049/cp:20070619

[13] Weinberg G, Alexopoulos A. Analysis of a dual order statistic constant false alarm rate detector. IEEE Transactions on Aerospace and Electronic Systems 2016; 52 (5): 2567-2574. doi: 10.1109/taes.2016.150508

[14] Weinberg G, Glenny VG. Enhancing Goldsteins Log-t Detector in Pareto-Distributed Clutter. IEEE Transactions on Aerospace and Electronic Systems 2017; 53 (2): 1035-1044. doi: 10.1109/taes.2017.2665144